



# Electrical source imaging in cortical malformation-related epilepsy: A prospective EEG-SEEG concordance study

\*†‡Estelle Rikir, §¶Laurent Koessler, \*\*†‡‡Martine Gavaret, \*\*†‡‡Fabrice Bartolomei, §§¶¶Sophie Colnat-Coulbois, \*§¶Jean-Pierre Vignal, \*§¶§Herve Vespignani, \*\*\*Georgia Ramantani, and \*§¶§Louis G. Maillard

*Epilepsia*, 55(6):918–932, 2014  
doi: 10.1111/epi.12591

## SUMMARY

**Objective:** Delineation of the epileptogenic zone (EZ) in refractory epilepsy related to malformations of cortical development (MCDs) often requires intracranial electroencephalography (EEG) recordings, especially in cases of negative magnetic resonance imaging (MRI) or discordant MRI and video-EEG findings. It is therefore crucial to promote the development of noninvasive methods such as electrical source imaging (ESI). We aimed to (1) analyze the localization concordance of ESI derived from interictal discharges and EZ estimated by stereo-EEG (SEEG); (2) compare the concordance of ESI, MRI, and electroclinical correlations (ECCs) with SEEG-EZ; and (3) assess ESI added value in the EZ localization.

**Methods:** We prospectively analyzed 28 consecutive patients undergoing presurgical investigation for MCD-related refractory epilepsy in 2009–2012. ESI derived from 64-channel scalp EEG was interpreted with blinding to, and subsequently compared with, SEEG-estimated EZ. Anatomic concordance of ESI with SEEG-EZ was compared with that of video-EEG and MRI. We further assessed ESI added value to ECC and MRI.

**Results:** Twelve patients (43%) had temporal and 16 (57%) had extratemporal epilepsy. MRI was negative in 11 (39%) and revealed a cortical malformation in 17 (61%). ESI was fully concordant with the EZ in 10 (36%) and partly concordant in 15 (53%). ECC presented a full and partial concordance with EZ in 11% and 82% of cases, respectively, and MRI in 11% and 46%, respectively. Of 11 patients with negative MRI, ESI was fully concordant with the EZ in 7 (64%) and partly concordant in 4 (36%). ESI correctly confirmed restricted or added localizations to ECC and MRI in 12 (43%) of 28 patients and in 8 (73%) of 11 patients with negative MRI.

**Significance:** ESI contributes to estimating the EZ in MCD-related epilepsy. The added value of ESI to ECC is particularly high in patients with MCD and negative MRI, who represent the most challenging cases for epilepsy surgery.

**KEY WORDS:** Electrical source imaging, Stereo-EEG, Malformations of cortical development.



Estelle Rikir is an epileptologist at the University Hospital, Liège, Belgium.

Accepted February 7, 2014; Early View publication April 4, 2014.

\*Neurology Department, University Hospital of Nancy, Nancy, France; †Neurology Department, University Hospital of Sart-Tilman, Liège, Belgium; ‡Medical Faculty, Liège University, Liège, Belgium; §CRAN, UMR 7039, Lorraine University, Vandœuvre-lès-Nancy Cedex, France; ¶CNRS, CRAN, UMR 7039, Vandœuvre-lès-Nancy Cedex, France; \*\*Clinical Neurophysiology Department, AP-HM, University Hospital la Timone, Marseille, France; ††INSERM UMR 1106, Institut de Neurosciences des Systèmes, Marseille, France; ‡‡Medical Faculty, Aix-Marseille University, Marseille, France; §§Medical Faculty, Lorraine University, Nancy, France; ¶¶Neurosurgery Department, University Hospital of Nancy, Nancy, France; and \*\*\*Epilepsy Center, University Hospital Freiburg, Freiburg, Germany

Address correspondence to Laurent Koessler, CRAN, UMR 7039, CNRS-Université de Lorraine, 2, Avenue de la forêt de Haye, Vandœuvre-lès-Nancy Cedex 54516, France. E-mail: laurent.koessler@univ-lorraine.fr

Wiley Periodicals, Inc.

© 2014 International League Against Epilepsy

Malformations of cortical development (MCDs) encompass a wide spectrum of congenital cortical structural abnormalities. They constitute one of the main causes of neocortical epilepsy.<sup>1</sup> Drug resistance is almost the rule and was recently estimated to concern 85% of patients with MCDs in a tertiary epilepsy center.<sup>2</sup> In those cases, surgical treatment provides the best results to achieve long-term seizure freedom,<sup>3</sup> and full resection of the epileptogenic zone (EZ) remains the main predictor of seizure freedom after surgery.<sup>3–5</sup> The EZ may be restricted to the malformation, extend to a network of remote cortical areas,<sup>6,7</sup> or involve only part of the malformation.<sup>7,8</sup> Therefore, precise estimation of the EZ associated with MCDs still often requires intracranial electroencephalography (iEEG)<sup>3,5</sup> or intracerebral EEG (stereo-electroencephalography, SEEG) recordings.<sup>6,7</sup> SEEG targets in MCDs are currently defined on the basis of electroclinical correlations (ECCs) and magnetic resonance imaging (MRI).<sup>9</sup>

There is a growing body of studies that have assessed the clinical value of additional imaging tools such as electric source imaging or magnetic source imaging (ESI, MSI)

derived from interictal discharges (IIDs) in the context of presurgical evaluation.<sup>10–17</sup>

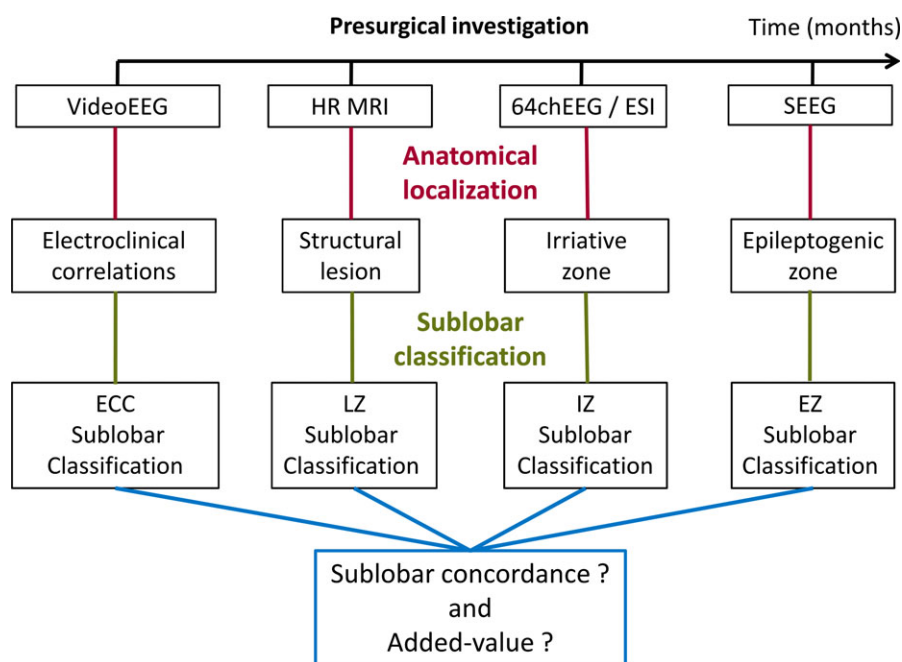
However, none of these studies specifically addressed the added value of these methods in the context of MCD-related refractory epilepsy. Past studies have focused on focal cortical dysplasia (FCD) or polymicrogyria (PMG), and were either retrospective<sup>18</sup> or not systematically validated against surgical outcomes or invasive EEG recordings.<sup>18–20</sup>

The *primary purpose* of this study was to prospectively evaluate the sublobar localization concordance of ESI derived from IIDs and EZ estimated by SEEG in MCDs. The *secondary purpose* of our study was to compare the concordance of ESI, MRI, and ECCs with SEEG-estimated EZ, and to ultimately assess the added value of ESI in the EZ localization of MCD-related drug-resistant partial epilepsy.

## MATERIALS AND METHODS

### Patient selection

Thirty consecutive patients with MCDs (26 from the University Hospital Nancy) were selected among a larger



**Figure 1.**

Consecutive steps of presurgical investigation. In a *first step*, the analysis of interictal and ictal video-EEG recordings led to electroclinical hypotheses regarding the anatomic topography of the EZ, which was then classified according to 18 predefined sublobar regions. In a *second step*, the analysis of the high-resolution MRI led to the determination of the anatomic localization of the LZ, which was then classified according to the same 18 predefined sublobar regions. In a *third step*, the analysis of the 64-channel EEG recordings and of the ESI led to the estimation of the anatomic localization of the IZ, which was then classified according to the same 18 predefined sublobar regions. In a *fourth step*, the analysis of the SEEG recordings led to the determination of the anatomic localization of the EZ, which was then classified according to the same 18 predefined sublobar regions. Finally, the sublobar localizations of ECC, LZ, and IZ were compared to those of EZ in order to determine their spatial concordance. EZ, epileptogenic zone; LZ, lesional zone; ESI, electrical source imaging; IZ, irritative zone; SEEG, stereo-electroencephalography; ECC, electroclinical correlations; HR MRI, high-resolution magnetic resonance imaging; 64 ch EEG, 64 channel EEG.

Epilepsia © ILAE

**Figure 2.**

Illustration of a case (patient 21) with negative MRI, full sublobar concordance of ESI and EZ, and confirmed ESI added value. **(A)** Hypothesis derived from long-term video-EEG recordings and ECC pointing toward the medial and lateral premotor and dorsolateral prefrontal areas. **(B)** MRI negative for structural lesions. **(C)** 64-Channel EEG recordings showed IID in channels AF3-F3-FC3 (monopolar montage, common average reference), correlating with sources localized in the depth of the left SFS and in the left MFG (ECD and sLORETA). These anatomic localizations corresponded to a dorsolateral prefrontal and lateral premotor sublobar classification. **(D)** SEEG recordings showed ictal discharges occurring first in the inferior part of the left SFS and the superior part of the left MFG (red square). CT-MRI co-registration shows the localization of the depth electrodes of interest. The red electrode recorded the inferior bank of SFS (internal contacts) and the superior part of MFG (external contacts). The middle and external contacts of the green electrode recorded the superior bank of SFS and the convexity of the SFG, respectively. The sublobar classification of EZ was consequently lateral premotor and dorsolateral prefrontal. **(E)** Considering the third column (sublobar classification), ESI was fully concordant with SEEG. ESI allowed a restriction of ECC that was validated by SEEG corresponding to an ESI added value. ECC, electroclinical correlations; IID, interictal discharge; 64 ch EEG, 64 channel EEG; ESI, electrical source imaging; ECD, equivalent current dipole; sLORETA, standardized low-resolution brain electromagnetic tomography; SEEG, stereo-electroencephalography; SFS, superior frontal sulcus; MFG, middle frontal gyrus; SFG, superior frontal gyrus; IFG, inferior frontal gyrus; EZ, epileptogenic zone; DMPref, dorsal medial prefrontal; DLPref, dorsal lateral prefrontal; MPrem, medial premotor; LPrem, lateral premotor.

*Epilepsia* © ILAE

cohort of 85 patients with drug-resistant partial epilepsy undergoing SEEG and prospectively enrolled between October 2009 and March 2012 in the multicenter National Clinical Research Project PHRC 2009-17-05, Clinical trial NCT 01090934 (Nancy, Marseille, Reims). We selected patients who were older than 15 years of age and had MRI or electroclinical findings consistent with MCDs. We excluded patients with a contraindication to SEEG. All patients with MCD-related refractory epilepsy who were undergoing presurgical investigations during this period were enrolled in the study, since all underwent an SEEG in order to delineate the EZ, to perform functional mapping and therapeutic thermocoagulation when indicated. This study was approved by the local ethics committee and all patients provided written informed consent.

**Noninvasive evaluation**

Noninvasive evaluation included comprehensive medical history, neurologic examination, long-term video-EEG recordings, high-resolution MRI, and neuropsychological evaluation in all cases, as well as optional interictal positron emission tomography (PET) and/or interictal/ictal single photon emission computed tomography (SPECT). We analyzed the ECCs, taking into account the interictal and ictal EEG findings as well as the ictal semiology, combining both interdependent modalities toward dynamic spatiotemporal hypotheses.<sup>9,21</sup> The sublobar localization of the presumed EZ according to ECC was consensually classified (LGM, JPV, and ER in Nancy; MG and FB in Marseille) in at least one of 18 predefined regions: ventral-medial prefrontal, dorsal-medial prefrontal, ventral-lateral prefrontal, dorsal-lateral prefrontal, medial premotor, lateral premotor, medial central, lateral central, medial-anterior temporal, lateral-anterior temporal, medial posterior temporal, lateral-posterior temporal, medial parietal, lateral parietal, medial occipital, lateral occipital, operculoincisor and temporo-parietooccipital junction (Figs. 1–4).

**MRI acquisition**

Structural MRI was acquired with a 1.5 or 3 Tesla Signa General Electric Medical System (GE Healthcare, Milwaukee, WI, U.S.A.) according to a standardized epilepsy protocol.<sup>22</sup> MRI scans were reviewed in a multidisciplinary case management conference by experienced epileptologists and neuroradiologists as to assess (1) the presence of MCDs and (2) the classification of their sublobar localization (Figs. 1–4).

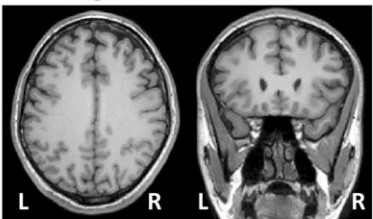

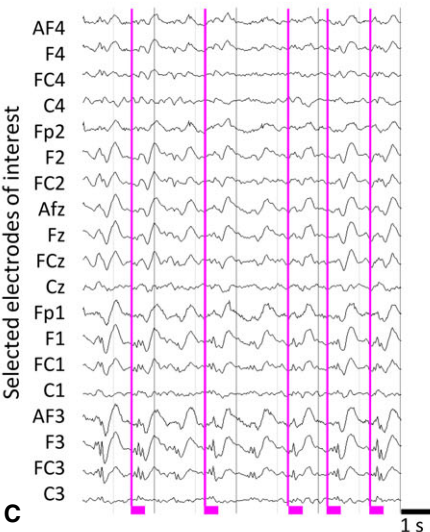
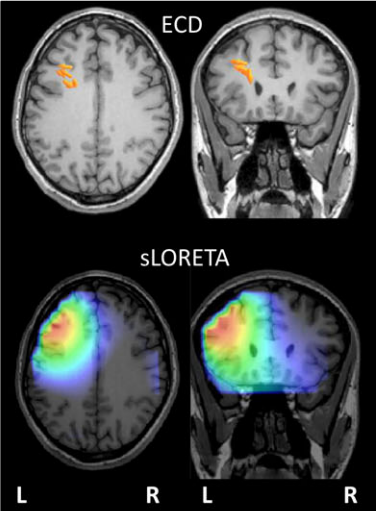

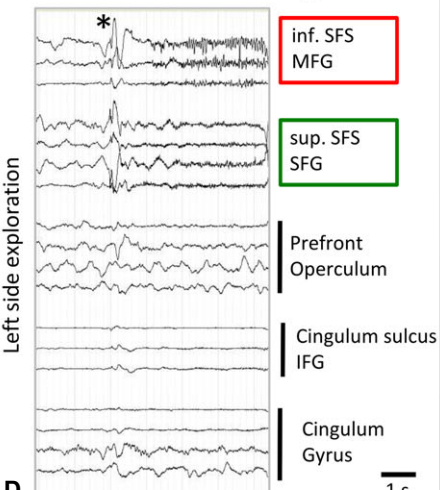
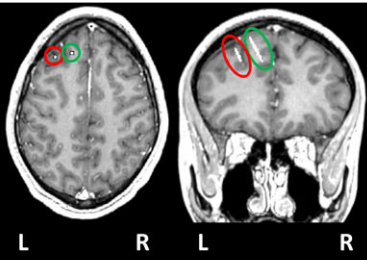

**64-Channel scalp video-EEG recordings and ESI***Acquisition*

EEG was recorded from 64 scalp-taped electrodes, placed according to the 10/10 system.<sup>23,24</sup> The localization of all 64 electrodes and of three fiducials (nasion and right and left tragi) was performed prior to acquisition either with a three-dimensional (3D) digitizer system (3Space Fastrak; Polhemus, Colchester, VT, U.S.A.) or with an automated detection and labeling system of MRI-visible sensors (ALLES).<sup>25</sup>

Electrode-skin impedance was below 5 k $\Omega$ . EEG was recorded with a 1,024 Hz sampling rate and a 0.53–400 Hz band-pass filter (University Hospital Nancy: Micromed, Mogliano Veneto, Italy; University Hospital Marseille: Del-tamed, San Carlos, CA, U.S.A.). The Fpz electrode generally provided the reference, except for frontal lobe cases, where the Oz electrode was used. Hyperventilation trials combined with antiepileptic drug (AED) tapering served to activate IIDs and seizures. Video-EEG was recorded for 4 days, 24 hours/day, in order to study interictal and ictal discharges. Two hours were selected for ESI after careful visual analysis of the full recording according to the following criteria: (1) absence of artifacts, (2) presence of calm wakefulness, and (3) presence of interictal discharges representative of all IID types.

*Interictal discharge detection and analysis*

Interictal spikes (<70 msec) and sharp waves (<200 msec)<sup>26</sup> were visually identified and marked in an

| Presurgical Investigations →  | Anatomical localizations →   | Sublobar classifications  |
|---|--|---|
| <b>A Ictal &amp; Interictal Video-EEG recordings</b><br><b>B High-resolution MRI</b><br> | <b>ECC: medial and lateral premotor - dorsal lateral prefrontal</b><br><br><b>Negative MRI</b>   |    |
| <b>C Interictal 64 ch EEG recordings</b><br>  | <b>ESI analysis</b><br>                                   |    |
| <b>D Ictal SIEG recordings</b><br>   | <b>SEEG analysis : electrodes involved in the EZ</b><br> |  |
|   |  | DM Pref<br>DL Pref<br>M Prem<br>L Prem<br>E   |

average reference montage by one of four experienced epileptologists (ER, LGM, JPV, or MG) according to the following established criteria<sup>27</sup>: (1) paroxysmal occurrence,

(2) abrupt change in polarity, (3) duration <200 msec, and (4) scalp topography consistent with a physiologic field. Temporal windows of analysis (max 100 msec) were



**Figure 3.**

Illustration of a case (patient 18) with discrepancy of ECC and MRI, full sublobar concordance between ESI and EZ, and confirmed ESI added value. **(A)** Hypothesis derived from long-term video-EEG and ECC pointing toward lateral and medial left premotor areas (L Prem, M Prem); **(B)** MRI showed a cystic enlargement of the collateral sulcus and raised suspicion of a glioneuronal lesion in the left temporal pole, corresponding to left medial and lateral anterior temporal sublobar classifications. **(C)** 64-Channel EEG recordings showed IID on channels AF7-F7-FT7-T3 (monopolar montage, common average reference) correlated with sources localized in the left temporal pole (ECD and sLORETA) suggesting epileptogenicity of the MRI-visible lesion. This anatomic localization matched to medial and lateral anterior temporal sublobar areas. **(D)** SEEG recordings showed ictal discharges occurring first in the left amygdala (green square), anterior hippocampus (red square), and temporal pole (blue square), confirming the epileptogenicity of the structural lesion. CT-MRI coregistration shows the localization of contacts of interest for each one of the depth electrodes involved in the EZ. The green electrode recorded the left amygdala (internal contacts) and MTG (external contacts). The red electrode recorded the left anterior hippocampus (internal contacts) and MTG (external contacts). The blue electrode recorded the left temporal pole and the structural lesion (internal and external contacts). The sublobar classification of EZ was consequently medial and lateral anterior temporal. **(E)** Considering the third column (sublobar classification), ESI was fully concordant with SEEG. ESI allowed a restriction of ECC that was validated by SEEG, corresponding to an ESI added value. This case illustrates that dense array EEG and ESI can contribute to determine the epileptogenicity of a lesion in case of discrepancy between ECC and MRI. ECC, electroclinical correlations; IID, interictal discharge; ECD, equivalent current dipole; sLORETA, standardized low-resolution brain electromagnetic tomography; 64 ch EEG, 64 channel EEG; ESI, electrical source imaging; SEEG, stereo-electroencephalography; EZ, epileptogenic zone; SMA, supplementary motor area; MAT, medial anterior temporal; LAT, lateral anterior temporal; MPrem, medial premotor; LPrem, lateral premotor; MTG, middle temporal gyrus.

*Epilepsia* © ILAE

defined around the IID and centered at the time of maximal negativity on the electrode trace with the highest amplitude (Advanced Signal Analysis/ASA software, Enschede, The Netherlands).<sup>11,14</sup> All 64 electrode traces were then superimposed to ascertain that the signal to noise ratio (SNR), defined as the highest IID amplitude divided by the highest background activity amplitude, was  $>2.5$ . For each patient, an average of 15 single IIDs were categorized according to their respective topography and morphology, and individually analyzed for source localization (range 1–4 IID types, average of 2 IID types by patient). We chose to analyze individual IIDs as opposed to averaged IIDs because of the risk of merging IID with comparable scalp cartography from different sources that is inherent in averaging.<sup>28</sup>

#### Volume conduction parameters

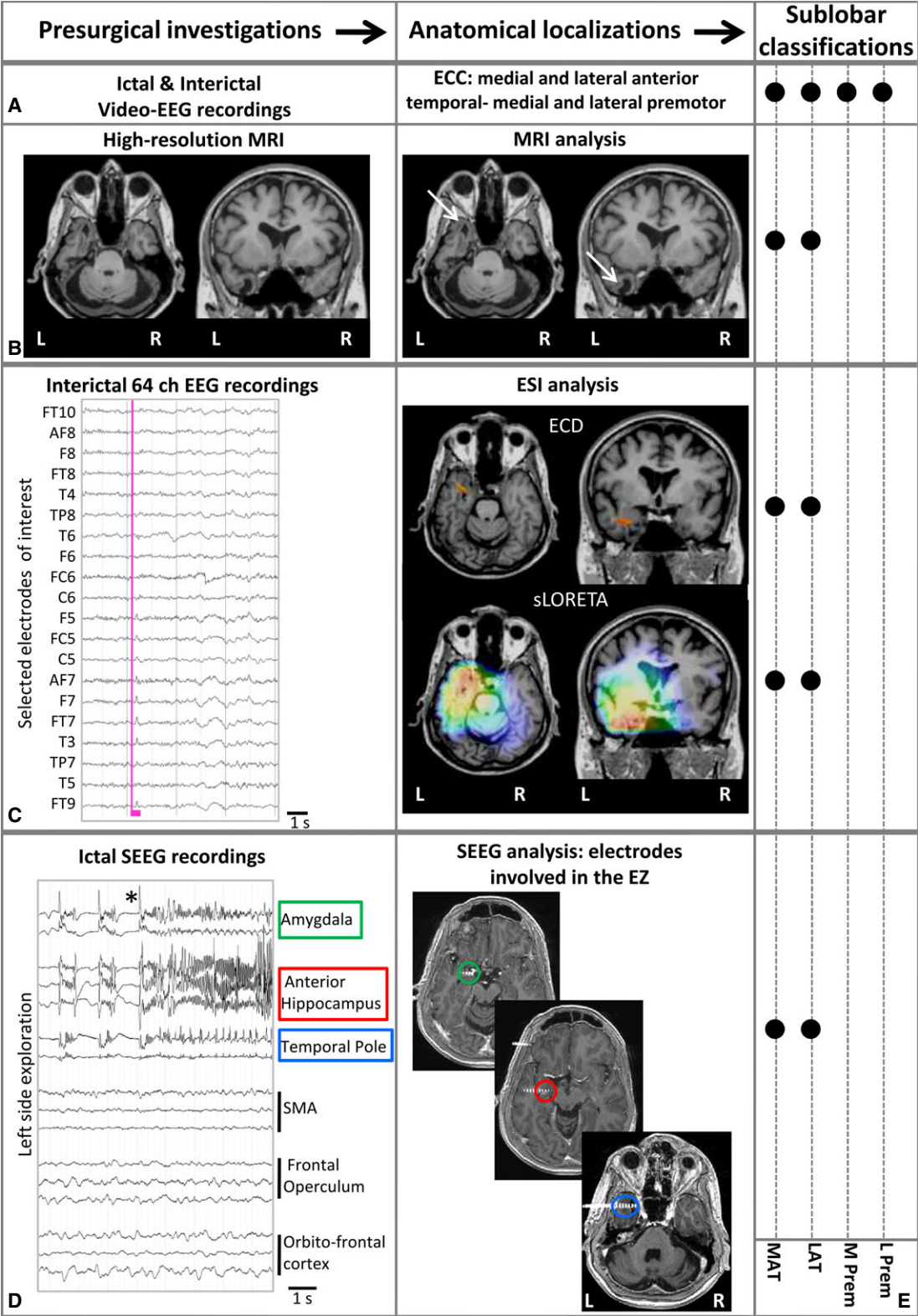
We chose to construct realistic head models for each patient because of evidence for lower ESI accuracy with spheric head models derived from a template MRI.<sup>10,29</sup> Realistic head models derived from an additional MRI sequence (3D BRAVO T<sub>1</sub>-weighted sequence with pixel size of 1.25 mm<sup>2</sup>, slice thickness of 1.25 mm without gaps between slices, 252 slices, matrix 192 × 192, field of view of 23 cm, Signa 1.5 Tesla, GE Healthcare). Coregistration of EEG and MRI data derived from the identification of the same three fiducials (nasion and right and left tragi). We performed a semiautomatic segmentation by ASA software that consisted of the identification of three isoconductivity compartments (scalp, skull, and intracranial space), with the skull estimated by the dilation of the intracranial space. We generated a realistic individual head model by the boundary element method (BEM), which describes each of three individual surfaces by triangulation using about 1,700–2,000 nodes per model.<sup>14</sup> We subsequently calculated an electric matrix with a conductivity

of 0.008 S/m for the skull and 0.33 S/m for the brain and scalp (conductivity ratio of skull to scalp = 1/40).<sup>30</sup>

#### Inverse problem methods

Intracerebral sources of each selected IID were modeled by both *equivalent current dipole* (ECD) and distributed source methods.<sup>31,32</sup> The ECD analysis was performed over the full duration of the selected temporal window with a *moving dipole*, involving the calculation of a new dipole localization, orientation, and amplitude that best reproduces the measured electric field for each millisecond, as well as with a *rotating dipole*, involving the calculation of a unique dipole localization across the time window of analysis. The localization of the moving dipole was considered optimal at the time point where goodness of fit (GOF), reflecting the percentage of EEG data explained by the model, was maximal, generally corresponding to the IID peak with maximal amplitude ratio. Stability of the source over the course of the IID ascending phase and peak was also assessed. No noise floor regularization was done with ECD models. Noise was estimated by the SNR ratio.<sup>14</sup>

We further applied a MultipleSignal Classification Method (MUSIC) that uses a 3D *dipole* grid (10 mm) model placed in the brain volume combined with the principal component analysis (PCA) method<sup>33</sup> and the standardized low-resolution brain electromagnetic tomography (sLORETA) procedure that relies on a *distributed* source model<sup>31,32</sup> to provide a 3D activity distribution over time. For MUSIC, noise floor regularization was performed using the PCA decomposition on the time window of analysis and the selection of the eigenvectors (dipoles), which explain 95% of the signal subspace. For sLORETA, we used the interval window for which we computed the inverse solution to estimate the noise floor. Noise was assumed to be independent in each sensor and taken into account using regularization



parameter. In our study, regularization was estimated via Generalized Cross Validation based on “leave one out” method.<sup>14,32</sup>

*Determination of the irritative zone by ESI*  
Two experienced epileptologists (LGM and JPV in Nancy; MG and FB in Marseille) prospectively and inde-

pendently interpreted the ESI results in the individual anatomic space for each selected IID and each patient in order to localize the irritative zone (IZ). In the event of discordance between the two interpreters, further joint analysis led to consensus.

The anatomic localization of each source was obtained from the coordinates of moving and rotating dipoles with GOF >90%, of the equivalent dipoles explaining >95% of the signal (eigenvector decomposition) using MUSIC, and of the dipoles with the highest magnitude using sLORETA. For each IID type and each source model, only reproducible localizations were considered relevant. In case of discordance between source models, we solely considered the models that yielded the most reproducible solutions for each IID type. These reproducible anatomic localizations were then classified according to the same 18 predefined sublobar localizations used for ECC and MRI (Figs. 1–4). In the event of multifocal IIDs, each corresponding and reproducible source was anatomically classified. There were 1–4 (mean 2) IID types per patient. This step was performed several months prior to SEEG and therefore epileptologists were blinded to its results.

### SEEG recordings and analysis

Intracerebral depth electrodes (Nancy: Dixi Medical, Besançon, France; Marseille: Alcis, Besançon, France) consisting of 5–15 contiguous contacts (length 2 mm, interval 1.5 mm) were stereotactically placed under general anesthesia.<sup>14</sup> A postsurgical computerized tomography (CT) scan performed to rule out hemorrhage was fused with the presurgical MRI to determine depth electrode positions.

SEEG was recorded 20 hours a day for 5–7 days under the same conditions as 64-channel scalp EEG. Spontaneous and electrically induced seizures were analyzed by one of four experienced epileptologists (ER, LGM, JPV, or MG) to estimate the EZ, defined as “the anatomical location of the site of the beginning and of the primary organization of the epileptic discharge.”<sup>9</sup> SEEG-estimated EZ was then classified according to the same 18 predefined sublobar localizations applied to ECC, MRI, and ESI (Figs. 1–4).

### Primary purpose

#### *ESI and SEEG estimated EZ sublobar concordance*

The ESI and SEEG estimated EZ sublobar concordance was assessed and classified as *fully concordant*, *partly concordant*, or *discordant* for each patient. *Full concordance* corresponded with a complete matching between ESI and EZ sublobar localizations ( $ESI = EZ$ ). *Partial concordance* corresponded with a partial matching between ESI and EZ sublobar localizations and encompassed three different conditions: (1) ESI pointed to the full EZ as well as to additional sublobar localizations ( $ESI > EZ$ ); (2) ESI pointed only to some EZ sublobar localizations ( $ESI < EZ$ ); (3) ESI pointed

to some EZ sublobar localizations and to additional localizations outside the EZ ( $ESI > EZ$ ). ESI and EZ were *discordant* if they had no common sublobar localization ( $ESI \neq EZ$ ; Figs. 2–4). In case of multifocal sources corresponding to multifocal IIDs, if all sources were included in but did not fully match the EZ, ESI was considered partially concordant. If none of the sources corresponded to the EZ, they were considered discordant.

### Secondary purpose

#### *Comparison of ECC, MRI, and ESI sublobar concordance with SEEG estimated EZ*

We further assessed the sublobar concordance of ECC and MRI with SEEG-estimated EZ according to the same definitions as for ESI (Fig. 1). Cases with negative MRI were considered *discordant*. The sublobar concordance of ESI, MRI, and ECC were thus compared.

#### *ESI added value*

In case of *sublobar concordance* of ESI with the localizations resulting from ECC and MRI, ESI was considered to confirm these localizations. In case of *sublobar discordance* of ESI and the localizations resulting from ECC and MRI, ESI could either restrict or add localizations. ESI was considered to have an added value compared to ECC and MRI in cases where it correctly confirmed, restricted, or added valid localizations (using SEEG as reference method) to those obtained from ECC and MRI.

## RESULTS

### Patients

We enrolled 30 patients (11 female) with mean age 28 years at inclusion, including 4 from the University Hospital Marseille and 26 from the University Hospital Nancy. Two patients were excluded due to failure to record seizures in SEEG.

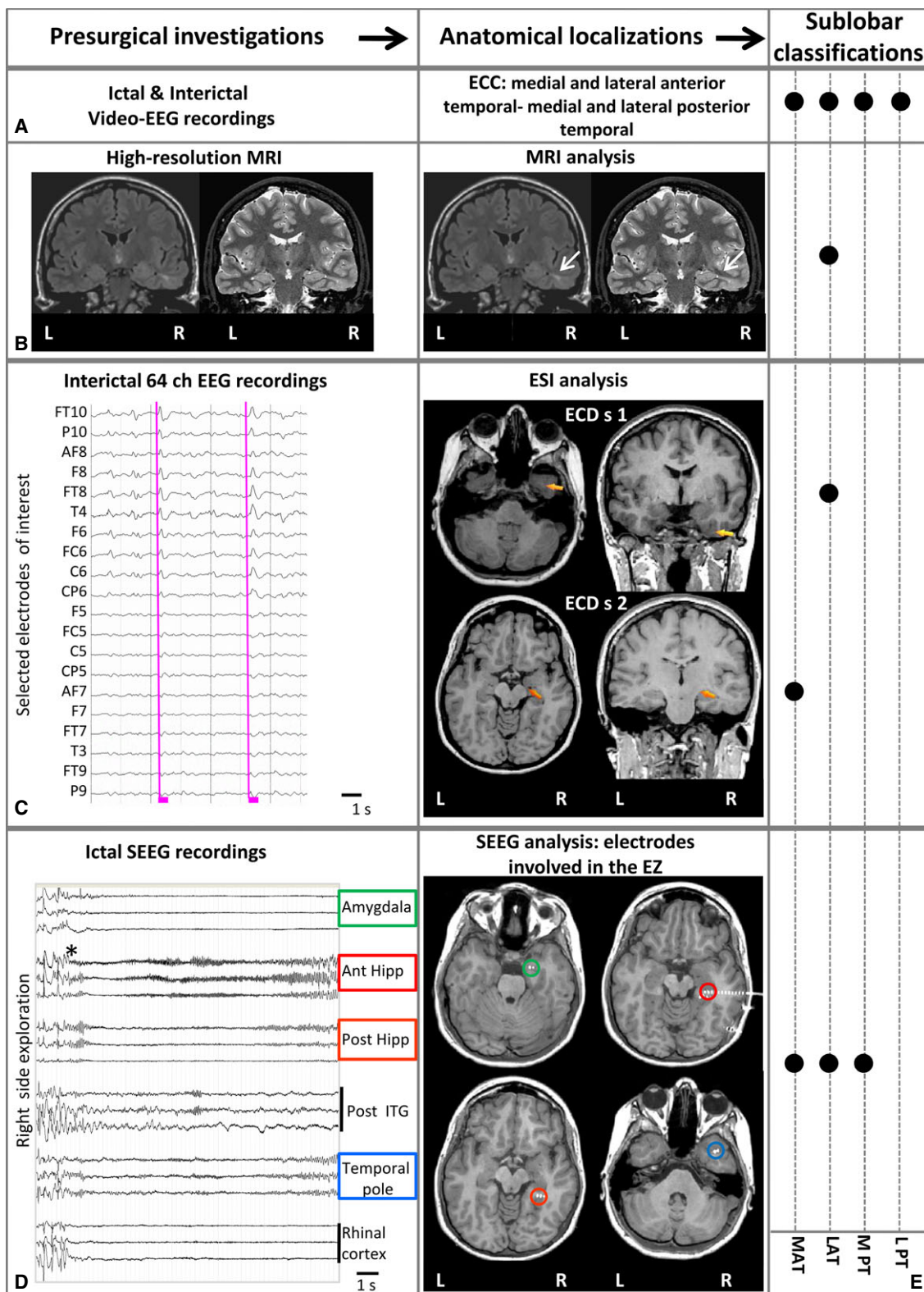
Twelve (43%) of 28 patients had temporal lobe epilepsy (TLE) and 16 (57%) had extratemporal epilepsy (ETLE): 12 (43%) frontal lobe epilepsy (FLE) and 4 (14%) posterior epilepsy, arising from the occipitotemporal or parietal regions.

MRI was negative in 11 patients (39%) and showed a lesion suggestive of MCD in 17 (61%), including FCD in 7 cases, dysembryoplastic neuroepithelial tumor (DNT) in 4, PMG with or without schizencephaly (SCZ) in 3, ganglioglioma in 2, and Bourneville tuberous sclerosis (TS) in a single case (Table 1).

### ESI and SEEG estimated EZ sublobar concordance

ESI and EZ were fully concordant in 10 patients (36%), including 7 MRI-negative cases (Figs. 2 and 3), partly concordant in 15 (53%) (Fig. 4), and discordant in 3 (11%).





Among the partly concordant cases: (1) ESI was entirely included into the EZ in 3 (ESI < EZ); (2) ESI entirely included the EZ in 6 (ESI > EZ); and (3) ESI and EZ partially overlapped in six patients (ESI >> EZ).

In the 11 MRI-negative patients, ESI was fully concordant with EZ in 7 and partly concordant in 4 patients. ESI was never discordant with EZ in this subgroup. Regarding the 17 patients with MRI evidence of MCD, ESI was fully



**Figure 4.**

Illustration of a case (patient 1) with partial sublobar concordance of ESI and EZ ( $ESI < EZ$ ). **(A)** Hypothesis derived from long-term video-EEG and ECC pointing toward the entire right temporal lobe. This anatomic localization corresponded to the medial and lateral anterior as well as medial and lateral posterior temporal sublobar areas. **(B)** MRI identified a suspected FCD in right inferior temporal gyrus (lateral anterior temporal sublobar classification). **(C)** 64-Channel EEG recordings showed IID on channels FT10-PI0-F8-FT8-T4-FC6-C6 (monopolar montage, common average reference) correlated with sources localized either in the temporal pole or in the anterior hippocampus (ECD). These anatomic localizations corresponded to medial and lateral anterior temporal sublobar localizations. **(D)** SEEG recordings showed ictal discharges occurring first in the amygdala (green square), the anterior and posterior hippocampus (red and orange squares), and the temporal pole (blue square). CT-MRI co-registration shows the localization of contacts of interest for each depth electrode involved by the EZ. The green electrode recorded the right amygdala (internal contacts) and the MTG (external contacts). The red electrode recorded the anterior hippocampus (internal contacts) and the MRI lesion and the MTG (external contacts). The orange electrode recorded the posterior hippocampus (internal contacts) and the MTG (external contacts). The blue electrode recorded the temporal pole (internal and external contacts). The sublobar classification of EZ was consequently medial and lateral anterior temporal but also medial posterior temporal. **(E)** Considering the third column (sublobar classification), ESI was partially concordant with SEEG and missed the medial posterior temporal area ( $ESI < SEEG$ ). ESI correctly restricted the posterior lateral temporal hypothesis derived from ECC but over-restricted the medial posterior temporal hypothesis. ECC, electroclinical correlations; FCD, focal cortical dysplasia; IID, interictal discharge; 64 ch EEG, 64-channel EEG; ECD, equivalent current dipole; SEEG, stereo-electroencephalography; EZ, epileptogenic zone; ESI, electrical source imaging; MTG, middle temporal gyrus; ITG, inferior temporal gyrus; MAT, medial anterior temporal; LAT, lateral anterior temporal; MPT, medial posterior temporal; LPT, lateral posterior temporal.

*Epilepsia* © ILAE

concordant with the EZ in 3 patients, partly concordant in 11, and discordant in 3. Overall, the full concordance rate amounted to 64% for MRI-negative patients and 18% for patients with MRI evidence of MCD.

In the 12 TLE patients, ESI was fully concordant with EZ in 3 (25%), partly concordant in 8 (67%), and discordant in 1 (8%). Regarding the 16 ETLE patients, ESI was fully concordant in 7 (44%), partly concordant in 7 (44%), and discordant in 2 (12%) (Table 2; see also Table S1).

#### **ECC MRI sublobar concordance with SEEG-estimated EZ**

ECC and EZ were fully concordant in 3 (11%), partly concordant in 23 (82%), and discordant in 2 patients (7%) (Table 2; see also Table S1). MRI and EZ were fully concordant in 3 (11%), partly concordant in 13 (46%), and discordant in 12 patients (43%), including 11 MRI-negative (Table 2; see also Table S1).

#### **ESI added value**

SEEG validated the confirmation of localizations by ESI in one of two cases, the restriction in 11 of 15. In the subgroup of 11 MRI-negative patients, ESI correctly restricted ECC in 8 cases. Regarding the 17 patients with MRI evidence for MCD, ESI correctly confirmed ECC and MRI in one case, correctly restricted ECC and MRI in 3.

ESI presented an added value in 12 (43%) of 28 patients. ESI added value was higher in the MRI-negative subgroup, where it correctly restricted sublobar localizations in 8 (73%) of 11 patients. In contrast, this added value was lower in the MRI-positive subgroup (4 of 17: 23%; Table 2). ESI added value was inferior in patients with temporal (4 of 12: 33%) compared to extratemporal (eight of 16: 50%) epilepsy.

## **DISCUSSION**

The purposes of this study were to prospectively evaluate the sublobar concordance of ESI and the SEEG estimated EZ in MCD-related epilepsy and to further assess its added value to video-EEG and MRI.

The strengths of our study entail (1) the prospective design and (2) the application of a uniform ESI methodology with 64-channel EEG recordings and realistic head models in all patients.

The overall sublobar concordance of ESI with the EZ is consistent with the previously reported ESI concordance rates of 84–94%.<sup>10,17</sup> Only three discordant cases were observed including one case with no detectable IID in scalp EEG (patient 28). In the two remaining cases, EZ localized in the lateral part of the right temporal lobe (case 5), or in the left lateral prefrontal area (case 12). In both cases, the EZ localizations over the convexity render a nonobservability of IID sources in scalp EEG improbable<sup>11,12</sup> and rather suggest a selection bias of IID (Table 1).

The relatively low rate of full concordance of ESI in our study (36%) may be related to the use of IIDs for ESI analysis, whereas the estimation of the EZ relied primarily on the analysis of ictal discharges.<sup>9</sup>

We identified an average of 2 IID types for each patient (range 1–4) corresponding to distinct sources. The partially concordant sources extending beyond the EZ corresponded to the SEEG-defined propagation zone in 10 of 12 cases. Therefore, our results suggest that the interictal sources located outside of the EZ mainly reflected the overlapping of the IZ with both the propagation and the epileptogenic zone.<sup>9,21</sup> We chose to consider the source with the highest GOF that corresponded to the IID peak in most cases.

Table 1. Clinical, neurophysiologic, neuroradiologic, and surgical data in the studied population

| Table 1. Clinical, neurophysiologic, neuroradiologic, and surgical data in the studied population |     |                  |                         |   |                     |  |               |                           |                |                         |                                |
|---|-----|------------------|-------------------------|---|---------------------|--|---------------|---------------------------|----------------|-------------------------|--------------------------------|
| Patient   | Sex | Age at inclusion | Type of epilepsy        | Ictal behavior (aura, initial objective ictal behavior)   | Number of IED types | Dominant channels  | Lesion on MRI | Surgery                   | Histopathology | Post-surgical follow-up | Outcome (Engel classification) |
| 1   | F   | 24               | r TLE                   | Anxiety; warns; verbal automatisms and OAA; postictal anomia  | 2                   | 1/FT10-F8-FT8-T8-F6-FC6-C6<br>2/FT8-T8-TP8                         | FCD           | Yes                       | FCD II         | 3 years                 | IA                             |
| 2   | F   | 28               | r TLE                   | Dreamy state; warns, OAA  | 2                   | 1/F8-FT8-T8-F6-FC6-C6<br>2/FT10-FT8-T8-TP8-C6-CP6                  | PMG/SCZ       | Yes                       | PMG/SCZ        | 3 years                 | IA                             |
| 3   | M   | 26               | r TLE                   | Auditory hallucination; warns; verbal automatisms   | 4                   | 1/F8-FT8-T8-3/F7-FT7-T7<br>4/T7-TP7-P7                             | DNT           | Yes                       | DNT            | 2.5 years               | IB                             |
| 4   | F   | 37               | r TLE                   | Ascending hot flush; warns; verbal automatisms and OAA, tachycardia                                 | 1                   | FT10-F8-FT8-T8   | PMG/SCZ       | Yes                       | PMG/SCZ        | 3 years                 | IA                             |
| 5   | F   | 26               | l TLE                   | Blurred vision and auditory illusion; warns: right-side eye and head deviation                      | 2                   | 1/TP8-P8-PO8<br>2/P8-CP6-P6  | DNT           | Yes                       | DNT            | 3 years                 | ID                             |
| 6   | M   | 29               | l FLE                   | Initial LOC; violent axial and UL automatisms, urinary need; postictal euphoria                     | 2                   | 1/Fp1-AF3-F3-F5-FC5<br>2/AF7-F7-FT7-FT9                            | FCD           | Yes                       | FCD II         | 2 years                 | IV                             |
| 7   | M   | 16               | l TLE                   | Initial LOC; IL automatisms; postictal anomia and dyslexia  | 2                   | 1/P7-PO7-PO3<br>2/P3-PO3-O1-P5-P7-PO7                              | DNT           | No for functional reasons | —              | —                       | —                              |
| 8   | M   | 28               | l TLE                   | Initial LOC; early OAA, staring; postictal anomia   | 1                   | AF7-F7-FT7-T7-F5-FC5-C5-FT9  | —             | Yes                       | FCD I          | 17 months               | IA                             |
| 9   | M   | 25               | r FLE                   | Warns; left IL then UL tonic flexion  | 2                   | 1/CP4-P4-CP6<br>2/C4-CP4-P4-C6-CP6-P6                              | FCD           | No for functional reasons | —              | —                       | —                              |
| 10  | F   | 32               | r Posterior (occipital) | Aura: visual hallucination; warns; right-side eye and head deviation, eyelid clonia                 | 4                   | 1/AF7-F7-FT7-T7-FT9<br>2/FT8-T8-TP8<br>3/P8-PO8-C6<br>4/P6-PO8-P10 | FCD           | No for functional reasons | —              | —                       | —                              |
| 11  | F   | 28               | l FLE                   | Aura: hot flush, palpitations; vegetative signs, violent axial motor automatisms, grasping movement | 3                   | 1/Fp1-F1-AF3-F3-AF7-F7-FT7<br>2/FC5-FT7-T7<br>3/F7-FT7-T7-FT9-P9   | —             | Yes                       | FCD I          | 20 months               | IV                             |
| 12  | M   | 30               | l FLE                   | Initial LOC; “chapeau de gendarme” grimace, eyelid clonia, eyeball elevation, OAA                   | 2                   | 1/Az-Fz-FCz-FC1-AF3-F3-FC3<br>2/Fp1-F5-FC5-AF7-F7-FT7-FT9          | TS            | Yes                       | TS             | 20 months               | ID                             |
| 13  | M   | 17               |                         |   | 4                   |  | —             | Yes                       | FCD            | 20 months               | ID                             |
| Continued   |     |                  |                         |   |                     |  |               |                           |                |                         |                                |

Continued

Table 1. Continued.

| Patient | Sex | Age at inclusion | Type of epilepsy               | Ictal behavior (aura, initial objective ictal behavior)  | Number of IED types | Dominant channels  | Lesion on MRI | Surgery                   | Histopathology | Post-surgical follow-up | Outcome (Engel classification) |
|---------|-----|------------------|--------------------------------|--|---------------------|--|---------------|---------------------------|----------------|-------------------------|--------------------------------|
| 14      | M   | 16               | I Posterior (parietal)         | Initial LOC; slow left-side eye and head deviation, right UL tonic abduction   | 2                   | 1/F1-FC1-AF3-F3-FC3<br>2/AF3-F3-FC3-F5-FC5<br>3/FC5-C5-AF7-F7-FT7<br>4/FT7-T7-TP7        | —             | Yes                       | FCD II         | 19 months               | IA                             |
| 15      | M   | 37               | b TLE                          | Initial LOC; right-side head deviation, left UL tonic flexion, smiling<br>Aura: bilateral auditory hallucinations; warns; fear behavior, OAA | 1                   | 1/F2-FC2-C2-F4-FC4-C4<br>2/F4-FC4-F6-FC6-C6<br>F6-FC6-C6-AF8-F8-FT8-T8-FT10              | —             | No                        | —              | —                       | —                              |
| 16      | F   | 43               | I Posterior (occipitotemporal) | Aura: vertigo; warns; eyelid clonia, complex oculomotor movement; postictal anomia   | 2                   | 1/T7-TP7-P7-CP5-P5<br>2/T7-TP7-P7-PO7-P9   | PMG/SCZ       | No for functional reasons | —              | —                       | —                              |
| 17      | F   | 25               | I FLE                          | Aura: head sensation; warns; left-side head deviation, right UL tonic extension or abduction, right facial clonic jerks                      | 2                   | 1/AF7-F7-FT7-F5-FC5-C5<br>2/C3-CP3-P3-PO3-C5-CP5-P5                                      | FCD           | Not yet                   | —              | —                       | —                              |
| 18      | M   | 48               | I TLE                          | Initial LOC; left-side head and eye deviation, grimace, right UL tonic abduction   | 1                   | FT9-F7-FT7-T7-TP7-P7-FC5-C5-CP5  | Ganglioglioma | Yes                       | Ganglioglioma  | 13 months               | IA                             |
| 19      | F   | 25               | r TLE                          | Aura: "déjà-vu", EAS; warns; right UL automatisms and OAA  | 2                   | 1/FT10-F8-FT8<br>2/F8-FT8-T8-F6-FC6  | DNT           | Yes                       | DNT            | 13 months               | II                             |
| 20      | M   | 23               | r FLE                          | Aura: ascending hot flush; warns; OAA, left UL tonic adduction followed by complex movements, left facial paresis, salivation                | 3                   | 1/FT10-AF8-F8-FT8-T8-F6-FC6<br>2/F8-F6-FC6-F4-FC4<br>3/F8-FT8-T8-F6-FC6-C6<br>AF3-F3-FC3 | Ganglioglioma | Yes                       | Ganglioglioma  | 13 months               | IA                             |
| 21      | M   | 22               | I FLE                          | Initial LOC; "chapeau de gendarme" grimace, right-side eye and head deviation  | 1                   | PI-CP3-P3-PO3-CP5-P5-PO5-P7  | —             | Yes                       | FCD II         | 12 months               | IA                             |
| 22      | M   | 33               | I Posterior (occipitotemporal) | Initial LOC; right brachiofacial tonic modifications, left UL automatisms; postictal anomia and right hemianopia                             | 1                   | —  | —             | No for functional reasons | —              | —                       | —                              |
| 23      | M   | 45               | I TLE                          | Initial LOC; OAA; postictal anomia and right facial paresis  | 2                   | 1/FT9-P9-F7-FT7-T7-TP7-P7<br>2/FT9-F7-FT7-T7-F5-FC5                                      | FCD           | Yes                       | FCD II         | 12 months               | IA                             |
| 24      | M   | 20               | r FLE                          | —  | 1                   | —  | —             | Not yet                   | —              | —                       | —                              |

Continued

Table 1. Continued.

| Patient | Sex | Age at inclusion | Type of epilepsy | Ictal behavior (aura, initial objective ictal behavior)  | Number of IID types | Dominant channels             | Lesion on MRI | Surgery | Histopathology | Post-surgical follow-up | Outcome (Engel classification) |
|---------|-----|------------------|------------------|--|---------------------|-------------------------------|---------------|---------|----------------|-------------------------|--------------------------------|
| 25      | F   | 21               | r TLE            | Warns: left-side head deviation, left UL tonic elevation followed by left UL and facial clonic jerks<br>Aura: auditory hallucination; warns: left-side head deviation<br>Aura: "déjà-vu" auditory illusion; warns: right face tonic modification | I                   | Fz-FCz-Cz-F1-FC1-C1-F2-FC2-C2 | —             | Yes     | Gliosis        | 7 months                | III                            |
| 26      | M   | 27               | l FLE            | Aura: "déjà-vu" auditory illusion; warns: right face tonic modification  | I                   | FC5-F5-CP5-FP1-AFz-FT7        | —             | No      | —              | —                       | —                              |
| 27      | M   | 21               | r FLE            | Aura: left shoulder twitches; warns: left-side head deviation, left brachiofacial tonic modification   | I                   | F2-FC2-Fz-FCz-AF4             | —             | No      | —              | —                       | —                              |
| 28      | M   | 38               | r FLE            | Aura: left ascending cold flush; warns: eyelid clonia, left-side eye deviation, euphoria   | 0                   | —                             | FCD           | Yes     | FCD I          | 3 years                 | III                            |

F, female; M, male; L, left; R, right; FLE, frontal lobe epilepsy; TLE, temporal lobe epilepsy; Posterior, posterior epilepsy; OAA, orolimentary automatisms; LOC, loss of consciousness; EAS, epigastric ascending sensation; UL, upper limb; IL, inferior limb; IID, interictal discharge; MRI, magnetic resonance imaging; FCD, focal cortical dysplasia; PMG, polymicrogyria; SCZ, schizencephaly; DNT, dysembryoplastic neuroepithelial tumor; TS, tuberous sclerosis.



**Table 2. Concordance of ECC, MRI, and ESI with SEEG-estimated EZ**

|                        | ECC                    |                        |                        |                              |                              | ECC                    |                         | ESI                                 |                                     | ESI                    |                         |
|------------------------|------------------------|------------------------|------------------------|------------------------------|------------------------------|------------------------|-------------------------|-------------------------------------|-------------------------------------|------------------------|-------------------------|
|                        | ECC<br>(n = 28)<br>(%) | MRI<br>(n = 28)<br>(%) | ESI<br>(n = 28)<br>(%) | MRI-negative<br>(n = 11) (%) | MRI-positive<br>(n = 17) (%) | TLE<br>(n = 12)<br>(%) | ETLE<br>(n = 16)<br>(%) | MRI-<br>negative<br>(n = 11)<br>(%) | MRI-<br>positive<br>(n = 17)<br>(%) | TLE<br>(n = 12)<br>(%) | ETLE<br>(n = 16)<br>(%) |
| Partial<br>Concordance | 82                     | 46                     | 53                     | 91                           | 76                           | 75                     | 88                      | 36                                  | 65                                  | 67                     | 44                      |
| Discordance            | 7                      | 43                     | 11                     | 9                            | 6                            | 8                      | 6                       | 0                                   | 17                                  | 8                      | 12                      |
| Full<br>concordance    | 11                     | 11                     | 36                     | 0                            | 18                           | 17                     | 6                       | 64                                  | 18                                  | 25                     | 44                      |
| Added-value            | —                      | —                      | 43                     | —                            | —                            | —                      | —                       | 73                                  | 23                                  | 33                     | 50                      |

ECC, electroclinical correlation; MRI, magnetic resonance imaging; ESI, electrical source imaging; TLE, temporal lobe epilepsy; ETLE, extratemporal lobe epilepsy.

Sources corresponding to IID peak have been presumed to reflect propagation, whereas those related to IID rising phase have been presumed to depict the EZ more reliably.<sup>34,35</sup> However, an analysis systematically restricted to the rising phase would have required averaging IIDs in order to increase their SNR,<sup>18</sup> entailing the risk of merging IID with comparable scalp cartography from different sources.<sup>28</sup>

Moreover, in our cohort, 75–100% of individually analyzed IIDs per patient showed a stable source over the superior part of the ascending phase (50% to the peak) with both moving dipole and sLORETA models. This suggests that the IID sources localized in the SEEG-defined propagation zone reflected propagated interictal spikes rather than the intrinsic spatiotemporal dynamic of individual spikes. The relatively low rate of full concordance might also be related to the choice of the reference method. We chose to rely on the SEEG estimation of the EZ because it is physiologically meaningful in the following: (1) validating another electrophysiological investigation, (2) differentiating the epileptogenic and propagation zones, and (3) including cases with a surgical contraindication for functional reasons, as was the case in five patients.

Beyond the issue of the ESI accuracy, it is crucial to determine the ESI added value that represents the cases where ESI correctly confirmed, restricted or added valid localizations (using SEEG as reference method) to those obtained from ECC and MRI.

ESI overall concordance (89%) was comparable to that of ECC (93%) and much higher than that of MRI (57%) because of the high rate of MRI-negative patients in our study. This can be primarily attributed to the focus on MCDs in our study. FCDs constitute the most frequent etiology of MRI-negative refractory neocortical epilepsy in adults.<sup>36</sup> In addition, the rate of ESI full concordance was much higher than that of ECC and MRI (36% vs. 11% and 11%, respectively). Indeed, ESI correctly focused or reinforced hypothesis derived from ECC and MRI in 43% of all

patients, meaning that ESI may facilitate ranking various hypotheses derived from video-EEG and MRI.

ESI-added value was higher for ELTE (50%) than for TLE (33%). This might be attributed to the use of 64 electrodes according to an adapted 10/10 international system that did not provide an optimal exploration of the basal temporal region.

The added value of ESI was varied according to the presence or absence of an MRI-visible lesion (23% vs. 73%). Although lower than in MRI-negative patients, the ESI-added value in MRI-positive subgroup was still meaningful in selected cases. In two of three cases with regional PMG (Table 1; see also Table S1), ESI contributed to correctly focus the hypothesis to the epileptogenic part of the malformation in one case (case 2)<sup>7</sup> and correctly pointed to a localization outside the visible lesion in another (case 4).<sup>8</sup> Moreover, in cases of ECC and MRI discrepancy, ESI contributed to determine the epileptogenicity of the MRI-detectable lesion (case 18; Fig. 3) or correctly localized the EZ outside of the visible lesion (case 4). In cases of more limited visible malformations such as FCD and DNT, the EZ may have either a focal lesion-centered or a network organization extending beyond the lesion.<sup>6</sup> In these cases, functional neuroimaging tools such as ESI or MSI can contribute to identify these *lesion-centered* or *network* organizations and to unravel the complex relation between lesion and EZ with sources either clustered in the vicinity of the dysplasia or scattered in remote cortical areas.<sup>20</sup>

The added value of ESI was especially relevant in MRI-negative patients (73%), in whom the EZ localization relies primarily on ECC. This higher accuracy most probably reflects the overlapping between irritative and epileptogenic zones observed in FCD<sup>4</sup> that constituted the etiologic substrate of the MRI-negative subgroup. In this subgroup, ESI primarily helped to rank the hypothesis and could thus contribute to appropriately focus the anatomic targets and guide the placement of intracerebral electrodes.

This higher accuracy of ESI in MRI-negative patients with MCD-related epilepsy is particularly important because this subgroup of refractory epilepsy patients has less favorable postsurgical outcomes, especially with respect to extratemporal epilepsy.<sup>37</sup>

Finally, there are some inherent limitations related to our study design. The first potential limitation concerns the smaller sample size, due to our prospective study design and the focus on MCDs, compared to a recent ESI study.<sup>10</sup> Our sample of 28 patients with MCD-related refractory epilepsy represented 33% of a larger prospective cohort that included 85 patients with refractory epilepsy of variable etiology. This is comparable to the 38% MCD rate in this previous study assessing the diagnostic value of ESI regardless of epilepsy substrate.<sup>10</sup> All patients with MCD-related refractory epilepsy undergoing presurgical investigations during this 29-month period underwent SEEG and were enrolled in this study. Altogether, this supports the absence of a selection bias toward cases of noncongruent or noncontributive video-EEG and/or MRI. Moreover, the sample size of our prospective study ( $n = 28$ ) far exceeds the average sample size ( $n = 14$ ) of previous retrospective studies assessing the contribution of ESI or MSI in MCD-related epilepsy work-up.<sup>18–20</sup> The second limitation is related to the use of 64-channel compared to 128- or 256-channel EEG recordings that allow a superior spatial sampling. These 64-channel EEG recordings with scalp-taped electrodes, as applied in our study, facilitate long-term sampling. Furthermore, a previous study comparing 31-, 64-, 128-, and 256-channel EEG recordings demonstrated that the most crucial step in increasing source-localization accuracy was related to the increase from 31 to 64 electrodes.<sup>38</sup> Therefore, 64-channel EEG recordings were performed as a viable compromise between dense array and clinical practice. The third limitation is related to the sampling bias of SEEG resulting from the partial coverage of the cortical surface.<sup>9</sup> SEEG estimation of the EZ was chosen as the reference method, as opposed to surgical volume, because it was physiologically meaningful in the following: (1) validating another electrophysiologic investigation, (2) differentiating the zone of seizure initiation from the zone of propagation, and (3) including cases with a surgical contraindication for functional reasons.

A previous retrospective study showed that PET may be useful in the identification of relevant SEEG targets and improve surgical outcome in MCD.<sup>39</sup> In the current study we did not assess the ESI added value compared to interictal PET because PET data were not prospectively collected and blindly analyzed. A previous study comparing ESI to PET in temporal lobe epilepsy suggests that ESI may present an added value to PET findings in MCD, by allowing hypometabolic areas to be distinguished related to initiation of IIDs from propagation areas.<sup>40</sup> This issue will have to be specifically addressed in a dedicated prospective study.

In conclusion, our prospective study showed that ESI combining data derived from 64-channel EEG recordings and from the individual anatomic MRI dataset had a higher concordance with SEEG-estimated EZ and a clinically relevant added value compared to scalp video-EEG and MRI for EZ estimation in MCD. ESI accuracy was particularly high in MRI-negative patients, who represent the most challenging subset of refractory epilepsy in term of EZ localization. Our results strongly suggest that ESI should improve the presurgical noninvasive evaluation of MCD-related partial refractory epilepsy. ESI provides valuable information regarding EZ localization that may improve the diagnostic yield of SEEG by identifying relevant SEEG targets and thus enhance the sampling of the suspected epileptogenic cortical regions.

## ACKNOWLEDGMENTS

This study was supported by the French Ministry of Health (PHRC 17-05, 2009). Estelle Rikir was supported by a grant from the Medical Council of the CHU of Liège, Belgium.

## DISCLOSURE

None of the authors has any conflict of interest to disclose. We confirm that we have read the Journal's position on issues involved in ethical publication and affirm that this report is consistent with those guidelines.

## REFERENCES

1. Spencer S, Huh L. Outcomes of epilepsy surgery in adults and children. *Lancet Neurol* 2008;7:525–537.
2. Papayannis CE, Consalvo D, Kauffman MA, et al. Malformations of cortical development and epilepsy in adult patients. *Seizure* 2012;21:377–384.
3. Chang EF, Wang DD, Barkovich AJ, et al. Predictors of seizure freedom after surgery for malformations of cortical development. *Ann Neurol* 2011;70:151–162.
4. Chassoux F, Devaux B, Landré E, et al. Stereoencephalography in focal cortical dysplasia: a 3D approach to delineating the dysplastic cortex. *Brain* 2000;123:1733–1751.
5. Krsek P, Maton B, Jayakar P, et al. Incomplete resection of focal cortical dysplasia is the main predictor of poor postsurgical outcome. *Neurology* 2009;72:217–223.
6. Aubert S, Wendling F, Regis J, et al. Local and remote epileptogenicity in focal cortical dysplasias and neurodevelopmental tumours. *Brain* 2009;132:3072–3086.
7. Ramantani G, Koessler L, Colnat-Coulbois S, et al. Intracranial evaluation of the epileptogenic zone in regional infratentorial polymicrogyria. *Epilepsia* 2013;54:296–304.
8. Maillard L, Koessler L, Colnat-Coulbois S, et al. Combined SEEG and source localisation study of temporal lobe schizencephaly and polymicrogyria. *Clin Neurophysiol* 2009;120:1628–1636.
9. Kahane P, Landré E, Minotti L, et al. The Bancaud and Talairach view on the epileptogenic zone: a working hypothesis. *Epileptic Disord* 2006;8(Suppl. 2):S16–S26.
10. Brodbeck V, Spinelli L, Lascano AM, et al. Electroencephalographic source imaging: a prospective study of 152 operated epileptic patients. *Brain* 2011;134:2887–2897.
11. Gavaret M, Badier JM, Marquis P, et al. Electric source imaging in temporal lobe epilepsy. *J Clin Neurophysiol* 2004;21:267–282.
12. Gavaret M, Badier JM, Marquis P, et al. Electric source imaging in frontal lobe epilepsy. *J Clin Neurophysiol* 2006;23:358–370.

13. Knowlton RC, Elgavish R, Howell J, et al. Magnetic source imaging versus intracranial electroencephalogram in epilepsy surgery: a prospective study. *Ann Neurol* 2006;59:835–842.
14. Koessler L, Benar C, Maillard L, et al. Source localization of ictal epileptic activity investigated by high resolution EEG and validated by SEEG. *Neuroimage* 2010;51:642–653.
15. Lantz G, Grave de PeraltaMenendez R, Gonzalez Andino S, et al. Noninvasive localization of electromagnetic epileptic activity. II. Demonstration of sublobar accuracy in patients with simultaneous surface and depth recordings. *Brain Topogr* 2001;14:139–147.
16. Merlet I, Gotman J. Dipole modeling of scalp electroencephalogram epileptic discharges: correlation with intracerebral fields. *Clin Neurophysiol* 2001;112:414–430.
17. Michel CM, Lantz G, Spinelli L, et al. 128-channel EEG source imaging in epilepsy: clinical yield and localization precision. *J Clin Neurophysiol* 2004;21:71–83.
18. Bast T, Oezkan O, Rona S, et al. EEG and MEG source analysis of single and averaged interictal spikes reveals intrinsic epileptogenicity in focal cortical dysplasia. *Epilepsia* 2004;45:621–631.
19. Bast T, Ramantani G, Boppel T, et al. Source analysis of interictal spikes in polymicrogyria: loss of relevant cortical fissures requires simultaneous EEG to avoid MEG misinterpretation. *Neuroimage* 2005;25:1232–1241.
20. Blenkmann A, Seifer G, Princich JP, et al. Association between equivalent current dipole source localization and focal cortical dysplasia in epilepsy patients. *Epilepsy Res* 2012;98:223–231.
21. Lüders H, Najm I, Nair D, et al. The epileptogenic zone: general principles. *Epileptic Disord* 2006;8(Suppl. 2):S1–S9.
22. Duncan JS. Neuroimaging in epilepsy: quality and not just quantity is important: current resources for neuroimaging could be used more efficiently. *J Neurol Neurosurg Psychiatry* 2003;73:612–613.
23. Koessler L, Maillard L, Benhadid A, et al. Automated cortical projection of EEG sensors: anatomical correlation via the international 10–10 system. *Neuroimage* 2009;46:64–72.
24. Oostenveld R, Praamstra P. The five percent electrode system for high-resolution EEG and ERP measurements. *Clin Neurophysiol* 2001;112:713–719.
25. Koessler L, Benhadid A, Maillard L, et al. Automatic localization and labeling of EEG sensors (ALLES) in MRI volume. *Neuroimage* 2008;41:914–923.
26. Walczak TS, Jayakar P, Mizrahi EM. Interictal encephalography. In Engel J Jr, Pedley TA (Eds) *Epilepsy – a comprehensive textbook*. 2nd Ed. Philadelphia: Wolters-Kluwer Lippincott Williams & Wilkins, 2008:809–823.
27. Chatrian GE. Report on the Committee on Terminology. Proceedings of the general assembly. The VIIIth international congress of electroencephalography and clinical neurophysiology. *Electroencephalogr Clin Neurophysiol* 1974;37:521–553.
28. Diekmann V, Becker W, Jurgens R. Localisation of epileptic foci with electric, magnetic and combined electromagnetic models. *Electroencephalogr Clin Neurophysiol* 1998;106:297–313.
29. Guggisberg AG, Dalal SS, Zumer JM, et al. Localization of corticoperipheral coherence with electroencephalography. *Neuroimage* 2011;57:1348–1357.
30. Gonçalves S, de Munck JC, Heethaar RM, et al. The application of electrical impedance tomography to reduce systematic errors in the EEG inverse problem—a simulation study. *Physiol Meas* 2000;21:379–393.
31. Hämäläinen MS, Ilmoniemi RJ. Interpreting measured magnetic fields of the brain: estimation of current distributions. Technical Report TKK-F-A559, Helsinki University of Technology, 1984:1–28.
32. Pascual-Marqui RD. Standardized low-resolution brain electromagnetic tomography (sLORETA): technical details. *Methods Find Exp Clin Pharmacol* 2002;24(Suppl. D):5–12.
33. Mosher JC, Lewis PS, Leahy RM. Multiple dipole modeling and localization from spatio-temporal MEG data. *IEEE Trans Biomed Eng* 1992;39:541–557.
34. Lantz G, Spinelli L, Seeck M, et al. Propagation of interictal epileptiform activity can lead to erroneous source localizations: a 128-channel EEG mapping study. *J Clin Neurophysiol* 2003;20: 311–319.
35. Ray A, Tao JX, Hawes-Ebersole SM, et al. Localizing value of scalp EEG spikes: a simultaneous scalp and intracranial study. *Clin Neurophysiol* 2007;118:69–79.
36. Hauptman JS, Mathern GW. Surgical treatment of epilepsy associated with cortical dysplasia: 2012 update. *Epilepsia* 2012;53(Suppl. 4):98–104.
37. Tomini C, Beghi E, Berg AT, et al. Predictors of epilepsy surgery outcome: a meta-analysis. *Epilepsy Res* 2004;62:75–87.
38. Lantz G, Grave de Peralta R, Spinelli L, et al. Epileptic source localization with high density EEG: how many electrodes are needed? *Clin Neurophysiol* 2003;114:63–69.
39. Chassoux F, Rodrigo S, Semah F, et al. FDG-PET improves surgical outcome in negative MRI Taylor-type focal cortical dysplasias. *Neurology* 2010;75: 2168–2175.
40. Merlet I, Garcia-Larrea L, Grégoire MC, et al. Source propagation of interictal spikes in temporal lobe epilepsy. Correlations between spike dipole modelling and [18F]fluorodeoxyglucose PET data. *Brain* 1996;119:377–392.

## SUPPORTING INFORMATION

Additional Supporting Information may be found in the online version of this article:

**Table S1.** Concordance of ECC, MRI, and ESI with SEEG-estimated EZ.